

## Earthquake observation of deeply embedded building structure

H. Matsumoto<sup>I</sup>, K. Ariizumi<sup>I</sup>, K. Yamanouchi<sup>II</sup>, H. Kuniyoshi<sup>II</sup>,  
O. Chiba<sup>III</sup>, and M. Watakabe<sup>III</sup>

### ABSTRACT

Earthquake observation of deeply embedded building structures in the suburbs of Tokyo has been continued on a large scale for the purpose of investigation of dynamic soil-structure interaction behavior. Many earthquake records have been obtained since June, 1985.

This paper introduces the outline of our earthquake observation system and the results obtained from the investigation of earthquake records observed in and around deeply embedded building structures and of dynamic lateral pressure acting on the basement walls.

- (1) The soil model for dynamic soil-structure interaction behavior subjected to earthquake ground motions is estimated by an identified technique which minimize the square sum of the residuals between the observed records and a simulated model. This soil model presented herein, closely simulates the observed records.
- (2) It is found that by comparison between the normalized spectra of the dynamic lateral pressure and those of the velocities at approximately the same depth, the both shapes of the spectra closely coincide.

### INTRODUCTION

Earthquake observation has been carried out at many building structures to investigate the dynamic soil-structure interaction behavior in Japan (Tsubokura et al. 1983, etc). Up till now, however, there has been little research related to the behavior of dynamic lateral pressures acting on the basement walls of deeply embedded building structures. In this paper, the authors wish to introduce the investigation of the fundamental characteristics of earthquake records observed in and around deeply embedded building structures and of the dynamic lateral pressure acting on the basement walls during earthquakes.

### OUTLINE OF EARTHQUAKE OBSERVATION SYSTEM

#### Outline of the ground, the building and observation system

Ground conditions around the building and cross-section of building are as

- I Engineering Research Center, Tokyo Electric Power Company, Tokyo, Japan
- II Architecture & Structural Technical Dept.,  
Tokyo Electric Power Services Co., Ltd., Tokyo, Japan
- III Institute of Construction Technology, Toda Corporation, Tokyo, Japan



summarized in Fig. 1(a),(b), respectively. Geological structure consists of soft alluvial deposits above thirty two meters and underlying diluvial deposits. About forty two meters below the ground surface, there exists a firm diluvial deposit, generally called the "Upper Tokyo Formation", which is selected as the bearing stratum of the building.

Earthquakes were observed with arrays set up inside the building and those set up vertically in the ground about one meter and about 12 meters from the building, respectively. Seismometers were installed in the building (4 sets, 12 components), in the ground about one meter from the basement wall (panel A) (3 sets, 9 components), and in the ground about 12 meters from the basement wall (panel D) (4 sets, 12 components). See Fig. 1(b). Dynamic earth and water pressures were observed during earthquake observation using 20 gauges (20 components) installed on the basement walls (See Fig. 1(b)).

#### Observed earthquakes

As of March 1990, many earthquakes have been observed since June 1985 when earthquake observation began. The locations of the epicenters of these earthquake are as shown in Fig. 2. For the purposes of this study, 21 earthquakes (Sakai et al. 1989) were chosen from earthquakes with an intensity of 2 or above in Tokyo (Japanese Meteorological Agency Scale) and a maximum peak acceleration value of  $3\text{cm/sec}^2$  or more observed at GL-142m.

### ANALYSIS OF OBSERVED RECORDS AND DISCUSSION

#### Observed records and maximum velocity distribution

The example of observed records of the East Off Chiba Prefecture Earthquake which occurred on December 17, 1987 is as shown in Fig. 3. The records observed in ground show a tendency that the velocity is hardly amplified between GL-142m and GL-42m, but it is amplified near the ground surface. Little amplification is observed between B6F and 1F of the building.

On the basis of observed records, the ratios of the maximum velocity at each observation point in the soil and in the building to the maximum velocity at GL-142m were determined. The mean values and standard deviations of the ratios obtained are as shown in Fig. 4. Both the horizontal and vertical components of velocity at GL-25.9m in the ground about 12 meters from the building were amplified by as low as 1.5 times on average. By contrast, they were more amplified above this level. Also, near the ground surface, the horizontal component was amplified by about 2.3 times on average and the vertical component by about 3.7 times on average. In the building, although amplification was observed at PH2, the horizontal component at B6F and 1F was amplified by as low as about 1.3 times and 1.5 times on average, respectively, indicating the effects on the embedment of the building.

#### Amplitude characteristics of the soil and the building

Correlation analysis was conducted on combinations of observed values obtained at two points in Array 1 as shown in Fig. 1, which was vertically set in the soil. The mean spectral ratios and standard deviations of GL-42m/GL-142m and GL-1.5m/GL-142m (horizontal component) were obtained as shown in Fig. 5(a) and (b), respectively, which represent transfer characteristics. Fourier spectra on smoothed by Parzen window having a bandwidth of 0.2 Hz are employed in this analysis. Fig.



5(a) shows that the primary frequency was predominant at around 0.71 Hz, while no predominance was observed in the secondary or higher mode of oscillation. In Fig. 5(b), predominance was observed at frequencies 0.71 Hz, 1.6 Hz, 2.56 Hz and 3.2 Hz, which indicated that predominant frequencies in higher modes of oscillation having a frequency of 1.60Hz or above were produced in shallow layers at GL-42m or above.

In order to investigate transfer characteristics between the ground and the building, the spectral ratio at each level was calculated using data observed in the ground at levels roughly corresponding to those observed at B6F and 1F. The results of this calculation are as shown in Fig. 6 (a) and (b), respectively. From the comparison between the spectrum at basement (B6F) and that in the soil layer at the depth of 25.9m, it is found that in the frequency range higher than the first natural frequency of the structure, the amplitude in the structure decreases to about half of that in the soil, and is accordance to the frequencies. The spectral ratio of 1F to GL-1.5m showed a similar tendency as estimated above. These phenomena indicated that dynamic soil-structure interaction occurred.

#### ESTIMATION OF SOIL MODEL BASED ON OBSERVATION RECORDS

##### The soil profile based on identified technique

A technique to minimize the square sum of the residuals between the observed records and the simulated model is employed, in which the shear wave velocities and the frequency-dependent damping factors are selected in accordance to the parameters, and the density and the layer thickness are set in accordance to the constant values. In the analysis, on the assumption that the soil consists of a multiple-layer horizontal formation, the amplitude characteristics were calculated by the one dimensional wave propagation theory. The soil constants for the initial soil model and the soil model estimated by the identified technique are as shown in Table 1. Example of the transfer characteristics obtained from the identified soil model and observed records are as shown in Fig. 7. As shown in the figure, predominant frequencies and amplitude characteristics of the soil model estimated by the identified technique showed close agreement with the observed ones.

##### Comparison of the results of observation and simulation

In order to evaluate the validity of the soil model estimated by the identified technique, simulation analysis was conducted. In the simulation analysis, the wave records observed at GL-142m were used as input. The example of comparisons of waveform and response spectrum (with a damping factor of 5%) between the observed and simulated waveforms are as shown in Fig. 8(a) and (b), respectively. In these figures, the simulated wave showed good agreement with the observed one. Although response spectrum values of the simulated wave at about 1.0 second were greater than the observed one, the simulated response spectrum showed good agreement with the observed one. Similar simulations were carried out for the remaining 20 earthquakes, and the ratios of response spectrum values of the simulated waves to those of the observed ones were calculated. The mean values and standard deviations are as shown in Fig. 9. It was confirmed that the average value of the simulations well agreed with the observed ones, despite greater standard deviations for periods of two seconds and more.

#### FUNDAMENTAL CHARACTERISTICS OF DYNAMIC LATERAL PRESSURE ON BASEMENT WALLS

##### Distribution of maximum dynamic lateral pressure



The mean values and standard deviations of the maximum dynamic lateral pressures on the basement walls are as shown in Fig. 10, in which the dynamic lateral pressure herein described signifies the fluctuation of earth pressure due to earthquake. The maximum dynamic lateral pressures shown in Fig. 10 are normalized by the maximum velocities at GL-142m. Fig. 11 shows variation coefficients between the maximum dynamic lateral pressures normalized by the maximum velocities and by the maximum accelerations at GL-142m, respectively. The variation coefficients of the maximum dynamic lateral pressures normalized by the maximum velocities are lower than those normalized by the maximum accelerations, and the variations in the vertical direction, smaller.

#### Time history and frequency characteristics of dynamic lateral pressure

The time history and frequency characteristics of dynamic lateral pressure which acts on the basement walls were investigated. The examples of dynamic lateral pressure at GL-3.2m on the panel A side and GL-3.7m on the panel D side, which were observed during the East Off Chiba Prefecture earthquake on December 17, 1987, are as shown in Fig. 12(a). The time history of dynamic lateral pressure is as shown in Fig. 12(b), in which the time history was passed through a band-pass filter (0.7 Hz-1.7 Hz) having a frequency bandwidth close to the predominant frequency of the Fourier spectra of dynamic lateral pressures as shown in Fig. 13. The time history obtained above (20-40 second in Fig. 12(a)) and an example of particle orbits are as shown in Fig. 12(b). Some phase difference was observed in the changes in dynamic lateral pressure acting on panels A and D.

Fourier spectra was normalized by the maximum values. These spectra consist of dynamic lateral pressures acting on panels A and D at the ground surface level and the foundation level, and of observed velocities at the corresponding levels of the soil. Their mean values and standard deviations are as shown in Fig. 13(a), (b) and (c), respectively. Spectra determined from observed dynamic lateral pressures showed good agreement with spectra of velocities observed at almost the same levels. This result indicates that observed dynamic lateral pressures and velocities were interrelated, though qualitatively.

#### CONCLUSIONS

Analysis on the fundamental characteristics of earthquake records observed in and around deeply embedded building structures was carried out and the following results have been obtained.

- (1) The amplification factor of the ground against GL-142m was as low as 1.5 or so on average (both horizontal and vertical) at GL-25.9m, while that at the ground surface level was about 2.3 (horizontal) and 3.7 (vertical) on average. The amplification factor of the building at the 6th basement level was about 1.3 (horizontal) on average, and that at the 1st floor level, about 1.5 on average. These results indicate the effects on the embedment of the building.
- (2) Spectrum ratios between the soil and the building at the levels of (1F/GL-1.5m) and (B6F/GL-25.9m) were examined. From comparison between the spectrum at basement (B6F) and that in the soil layer at the depth of 25.9m, it is found that in a frequency range higher than the first natural frequency of the structure, the amplitude in the structure decreases to about half of that in the soil, and is in accordance to the frequencies. The spectral ratio of 1F to GL-



1.5m showed a similar tendency as estimated above. These phenomena indicated that dynamic soil-structure interaction occurred.

- (3) It was confirmed that the soil model estimated by an identified technique assuming a frequency-dependent damping factor closely simulates the observed record. Therefore, it was confirmed that the soil model could be applied for further investigation of dynamic soil-structure interaction behavior.
- (4) The maximum dynamic lateral pressure requires a smaller variation coefficient and a smaller vertical variation when normalized by the maximum velocity than by the maximum acceleration. Examination of the time history and frequency characteristics of dynamic lateral pressure acting on basement walls revealed that there was some phase difference in dynamic lateral pressure acting on panels A and D at the ground surface level. Spectra determined from observed dynamic lateral pressures showed good agreement with spectra of velocities observed at almost the same levels. This result indicates that observed dynamic lateral pressures and velocities were interrelated, though qualitatively.

#### REFERENCES

Sakai, Y., et al. 1989. Earthquake Observation of Deeply Embedded Building (in Japanese). Annual Meeting of A.I.J., 267-268.

Tsubokura, H., et al. 1983. Observation and Analysis of Earthquake Motions to Deeply Embedded Underground Structure (in Japanese). Annual Meeting of A.I.J., 779-780.

Table 1 Data of soil profile

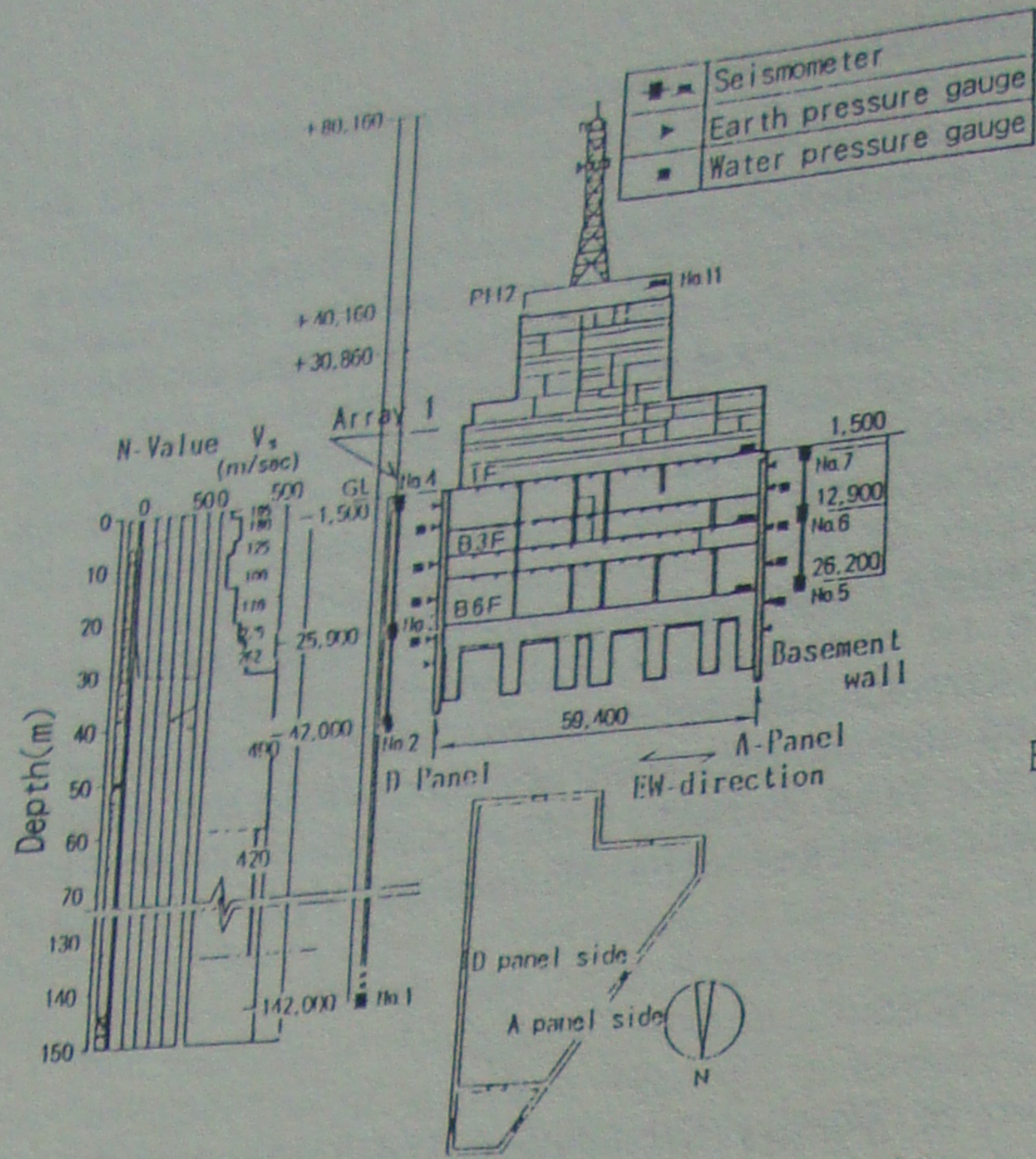
Observation points(m)	Thickness (m)	Density (g/cm <sup>3</sup> )	Initial model		Identified model		
			V <sub>s</sub> (m/s)	h(%)	V <sub>s</sub> (m/s)	h <sub>0</sub> * (%)	α
GL-1.5 ●	1.5	1.80	105.0	5.0	105.0	9.1	0.48
	2.3	1.80	180.0	5.0	147.0	9.1	0.48
	1.5	1.80	125.0	5.0	126.0	9.1	0.48
	7.6	1.58	100.0	5.0	131.0	9.1	0.48
	8.1	1.64	170.0	5.0	195.0	9.1	0.48
GL-25.9 ●	4.9	1.68	225.0	5.0	239.0	9.1	0.48
	6.2	1.69	262.0	5.0	230.0	9.1	0.48
GL-42.0 ●	9.9	1.80	490.0	5.0	410.0	10.3	0.66
	100.0	1.97	420.0	5.0	431.0	10.3	0.66
GL-142.0 ●	—	2.00	500.0	5.0	500.0	10.3	0.66

● Observation points

$$*: h(f) = h_0 \cdot f^{-\alpha}$$

where, α : Constant expressing the degree of dependence on frequency  
 h<sub>0</sub> : Damping factor at 1 Hz, f : Frequency (Hz)





(a) Soil profile (b) Location of observation points  
 Fig. 1 Outline of soil profile and building structure

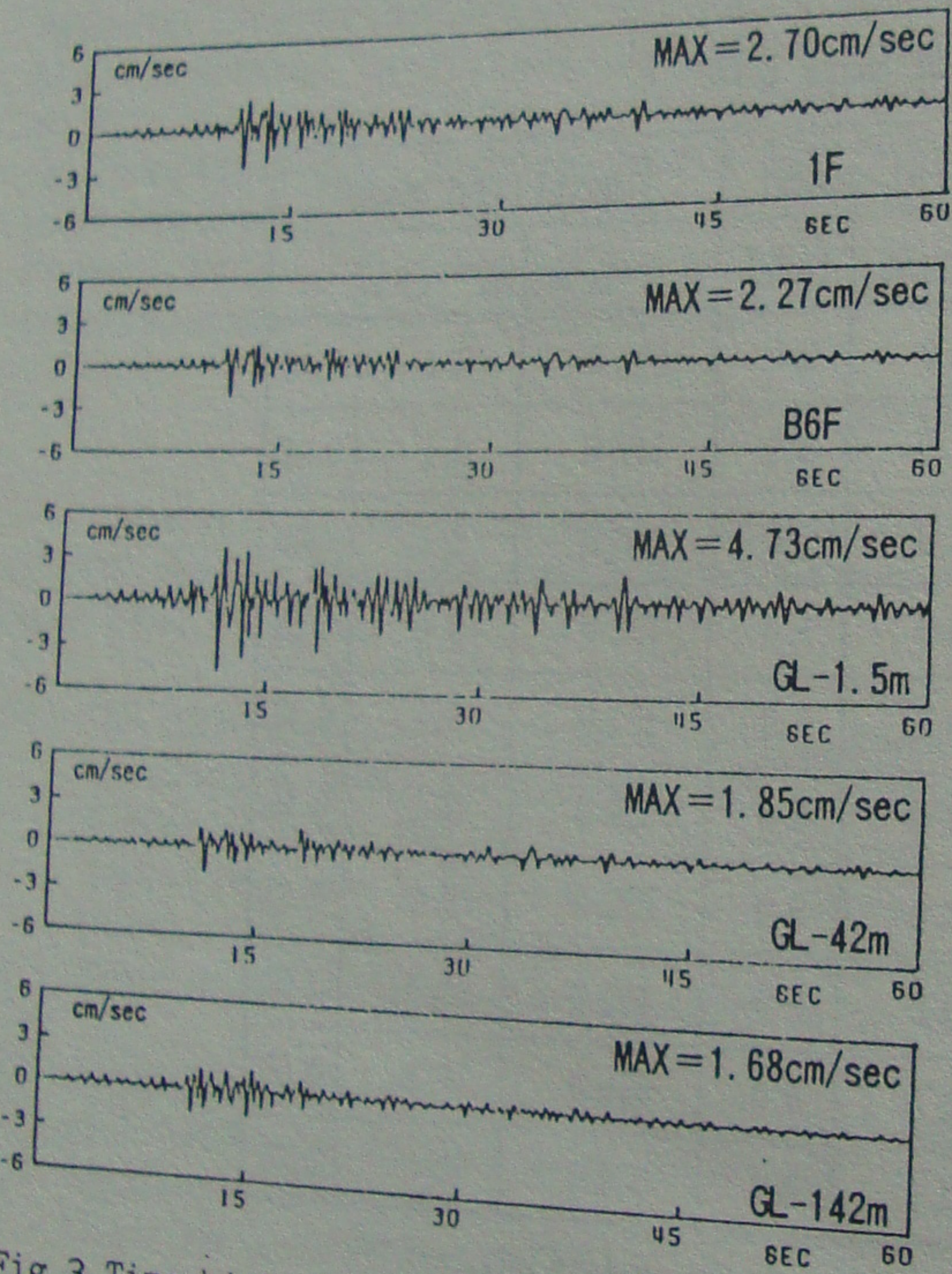


Fig. 3 Time histories observed during 1987 E-Off Chiba Prefecture Earthquake (NS component)

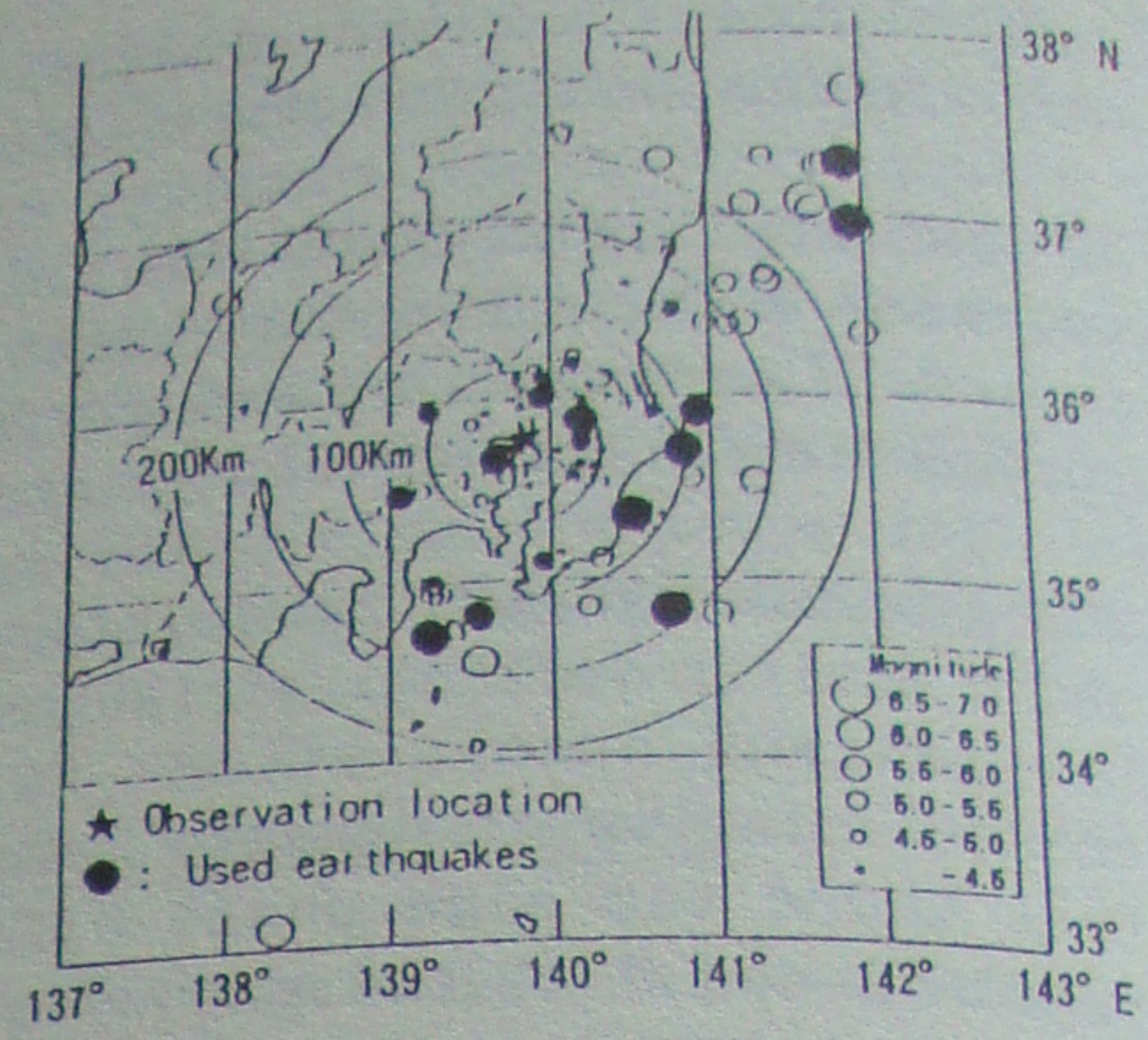


Fig. 2 Location of epicenter and magnitude for observed earthquakes

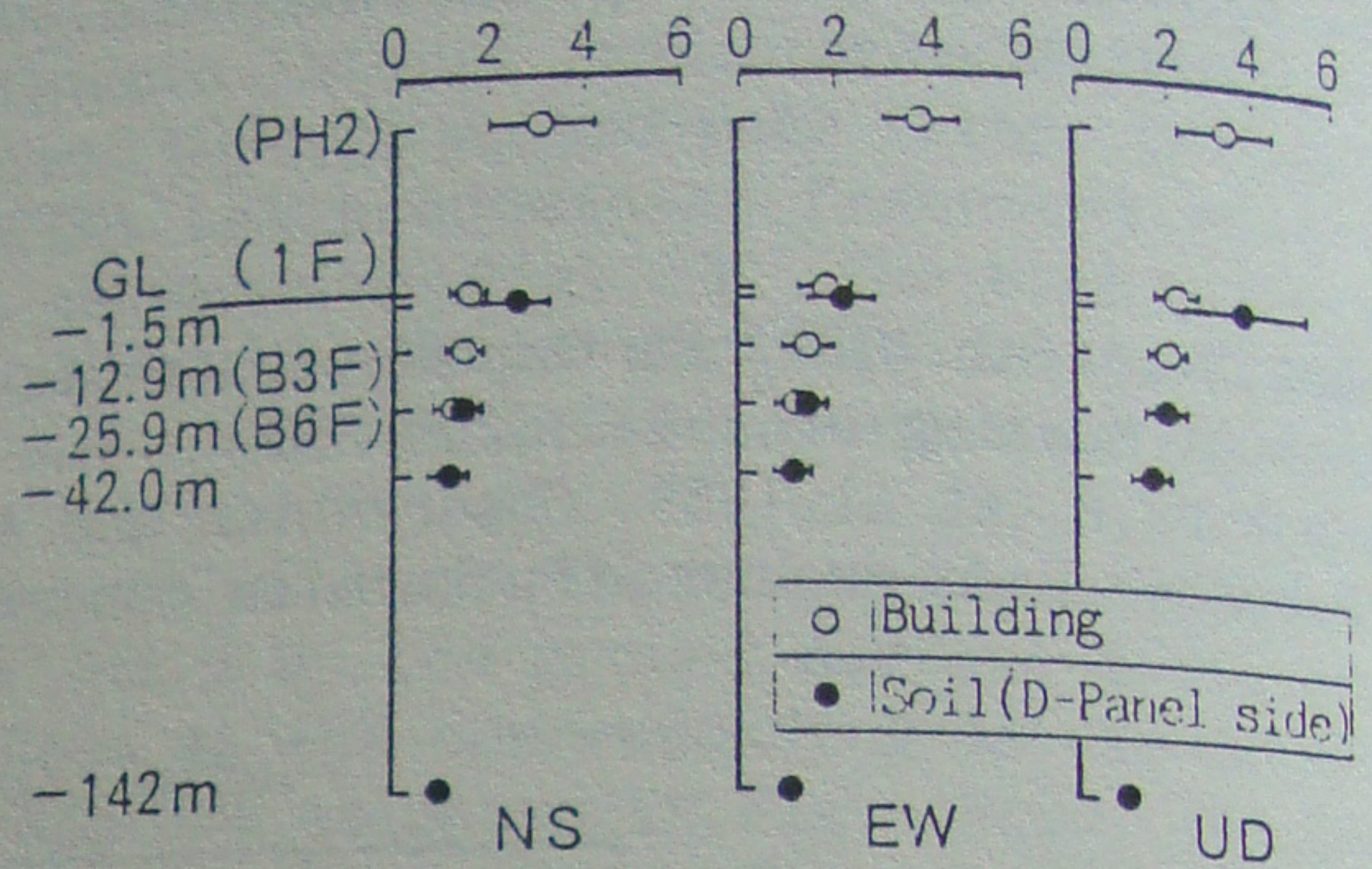


Fig. 4 Distributions of mean values and standard deviations of maximum velocity (Normalized by the maximum velocity at GL-142m)

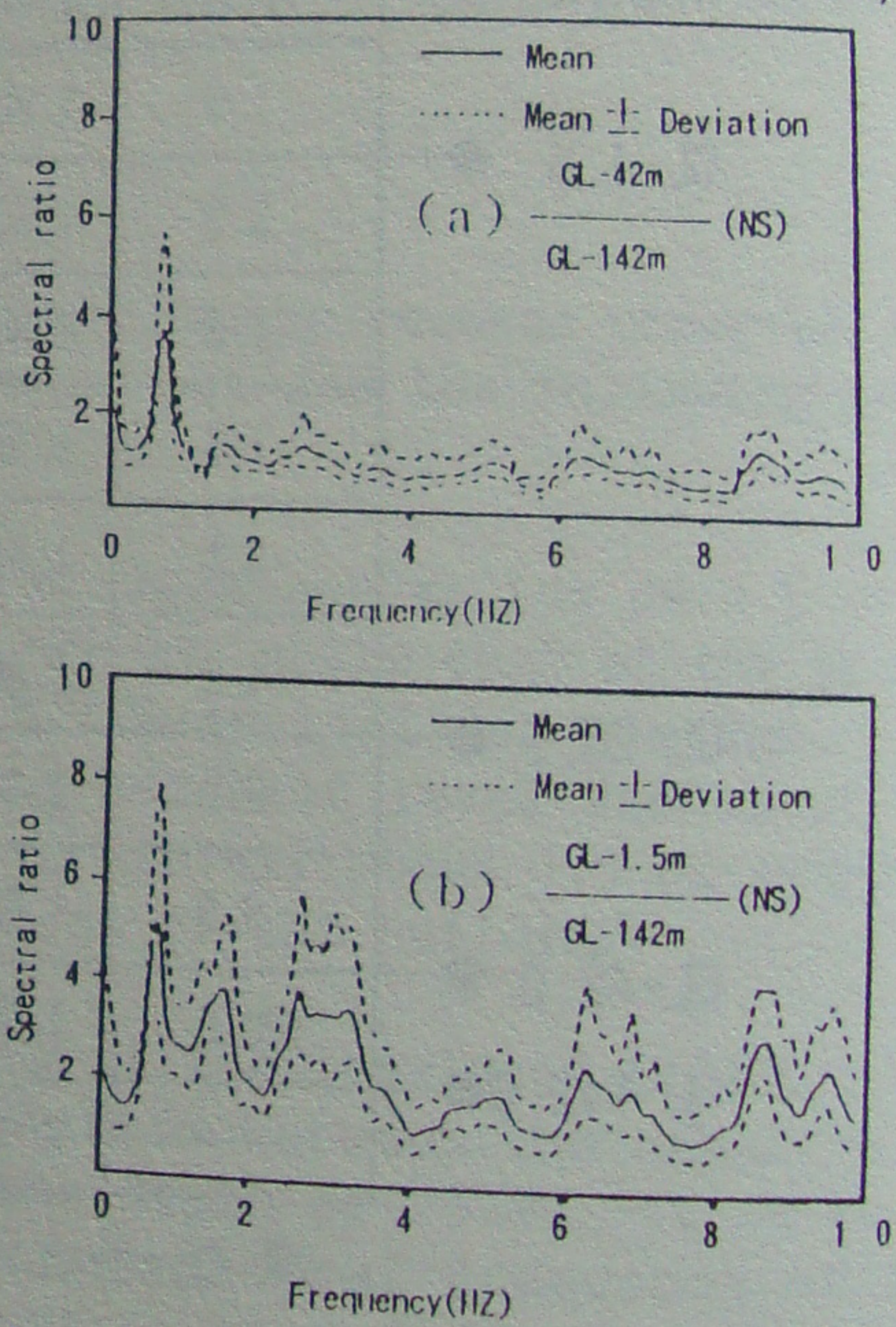


Fig. 5 Averaged spectral ratio of soil layer (NS-direction)



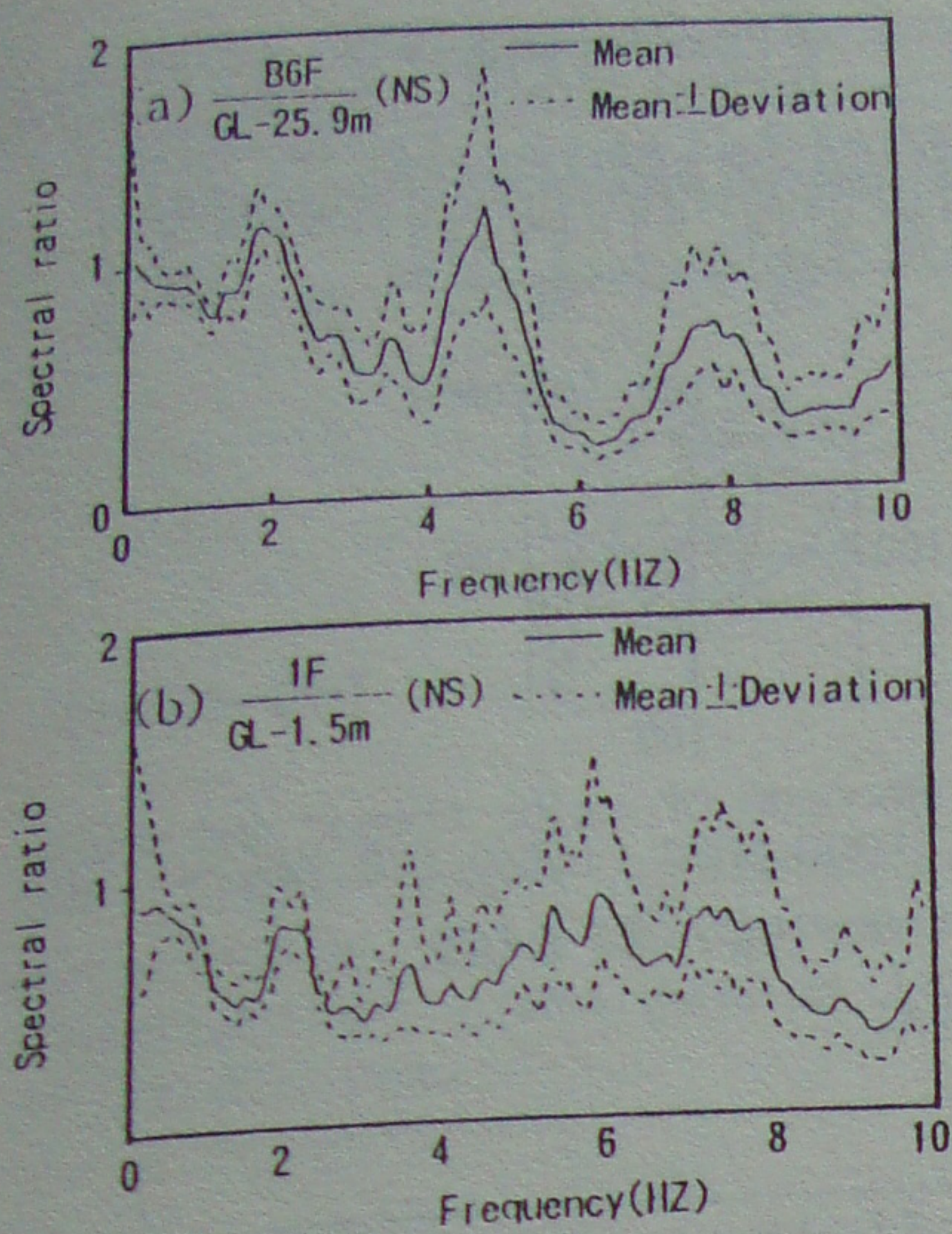


Fig. 6 Averaged spectral ratio obtained from observed records in the building and the surrounding soil

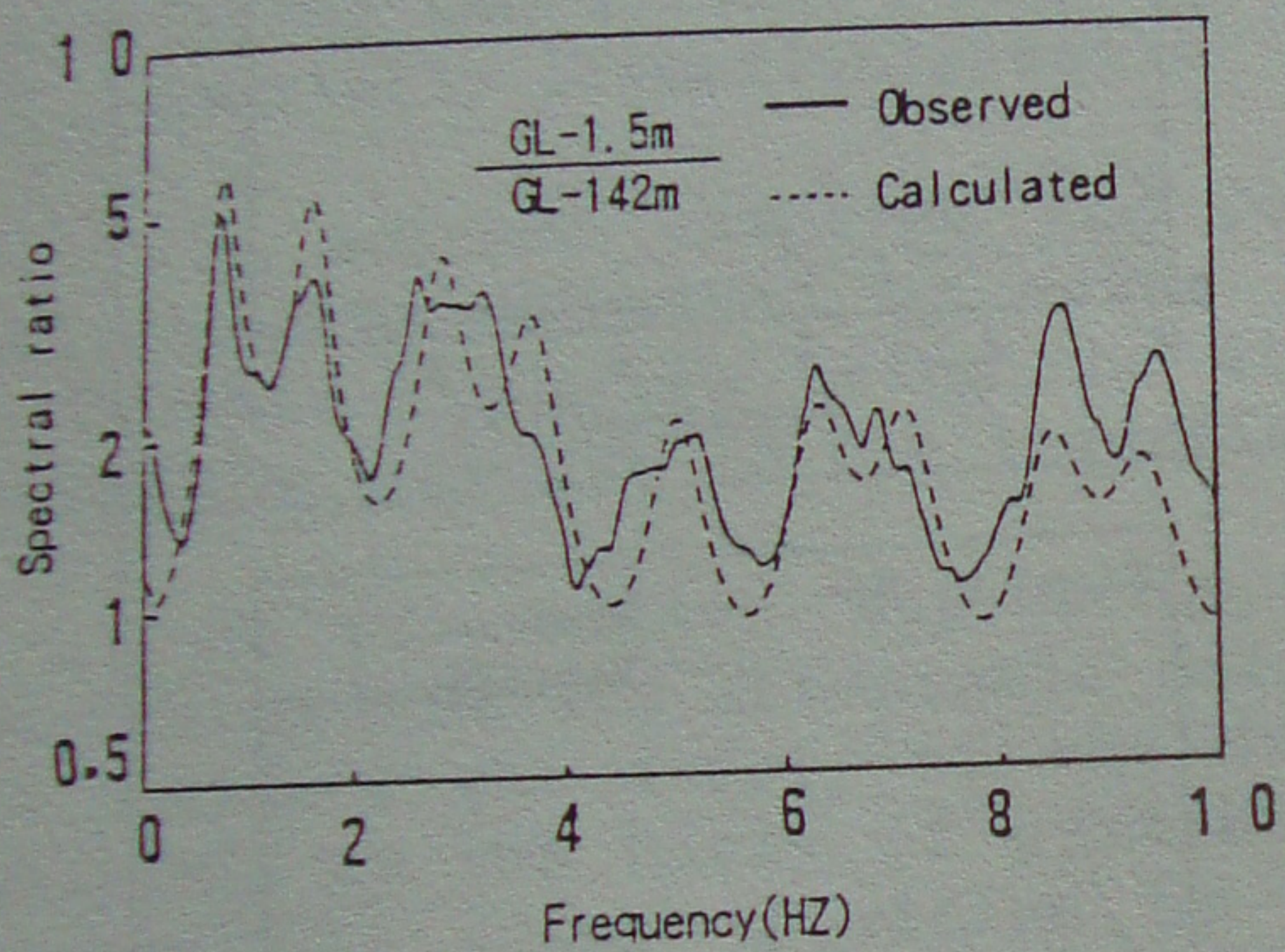


Fig. 7 Comparison of observed transfer function and theoretical one

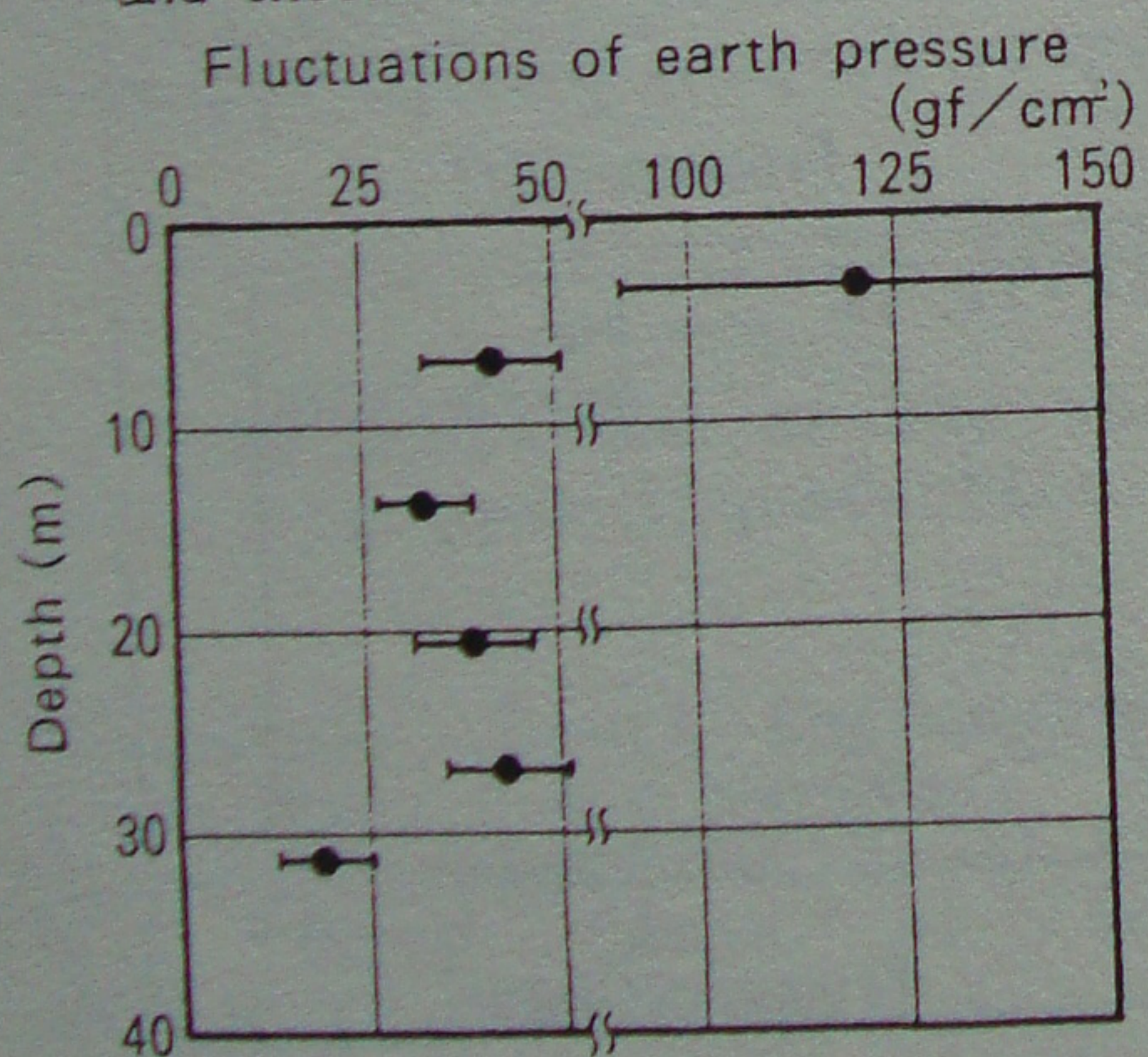
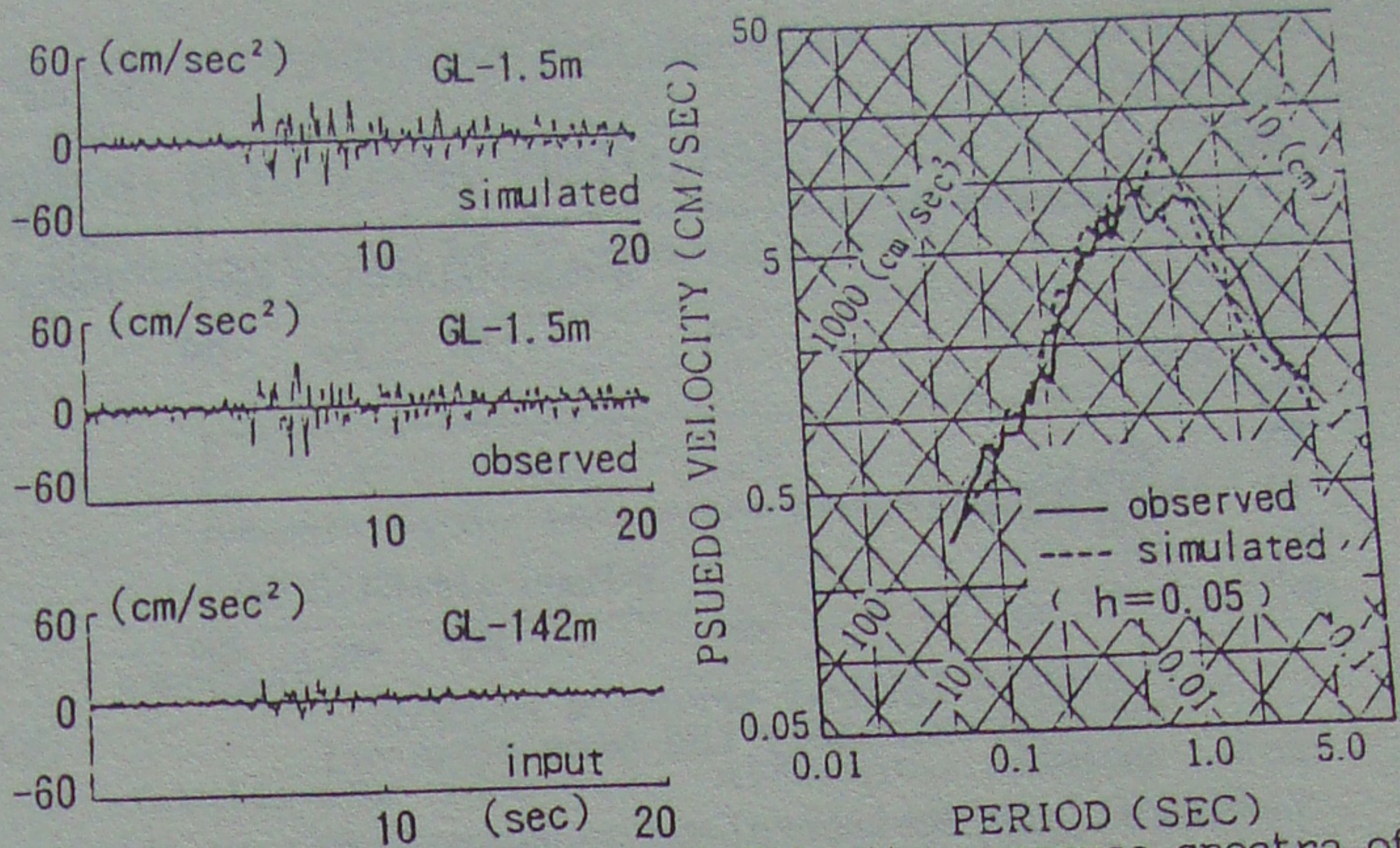


Fig. 10 Maximum dynamic lateral pressure distribution (mean and deviation)



(a) Simulated wave and observed wave at GL-1.5m (b) Velocity response spectra of simulated wave and observed record at GL-1.5m

Fig. 8 1985 Southern Ibaraki Prefecture Earthquake (M=6.2, Focal depth=76km, Epicentral distance=38km)

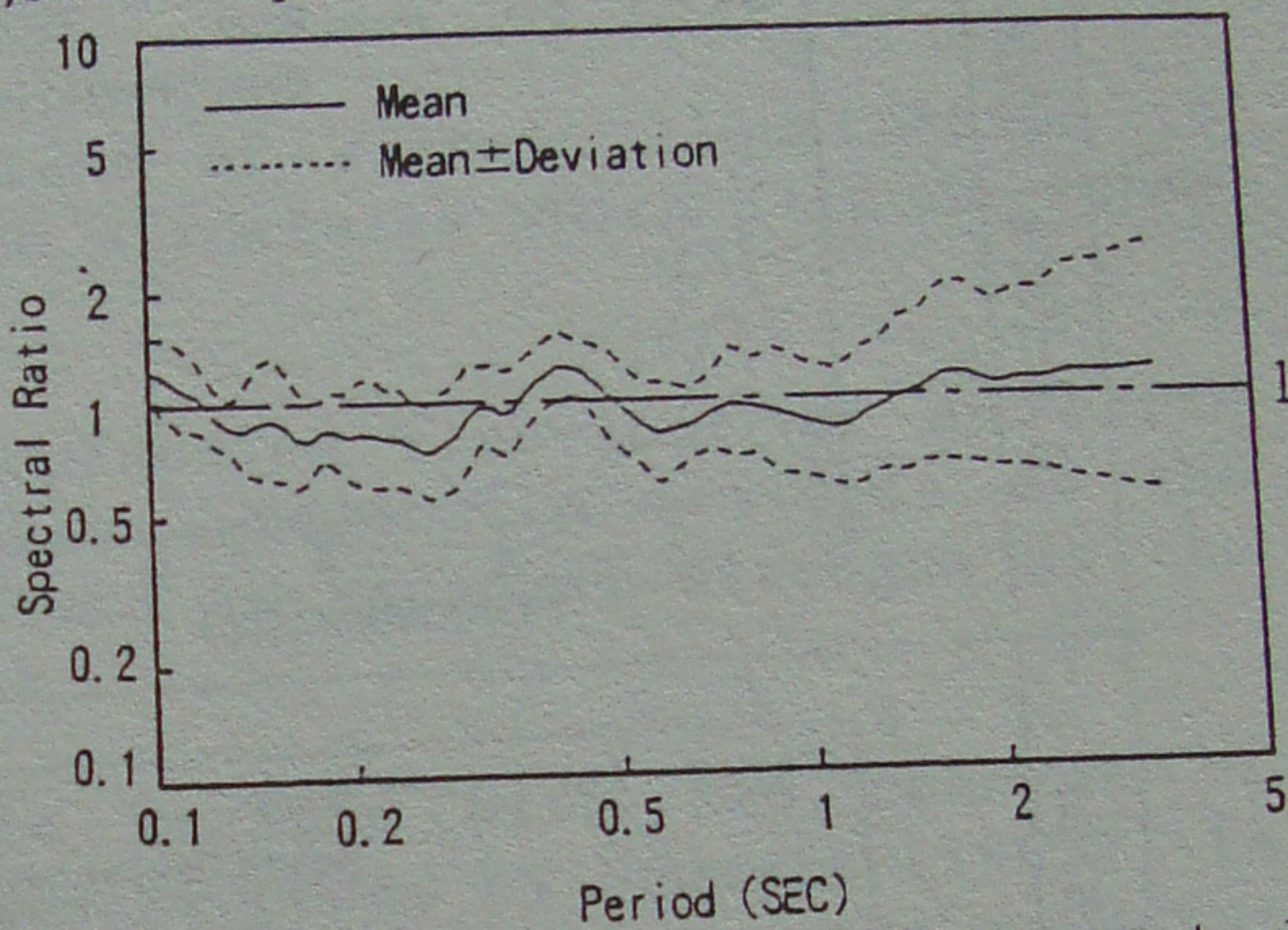


Fig. 9 Averaged velocity response spectral ratio at GL-1.5m (simulated/observed)

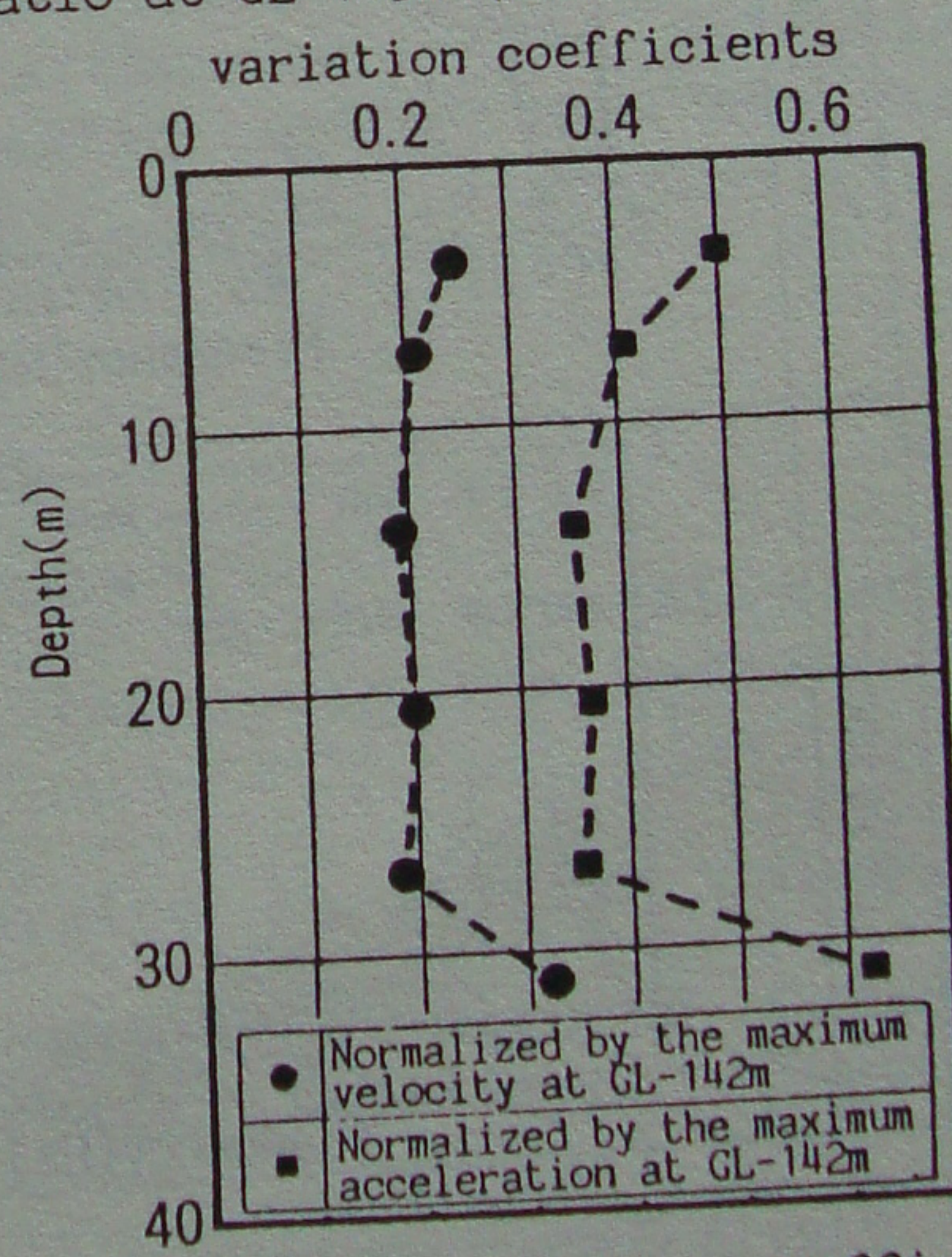


Fig. 11 Distribution of variation coefficients



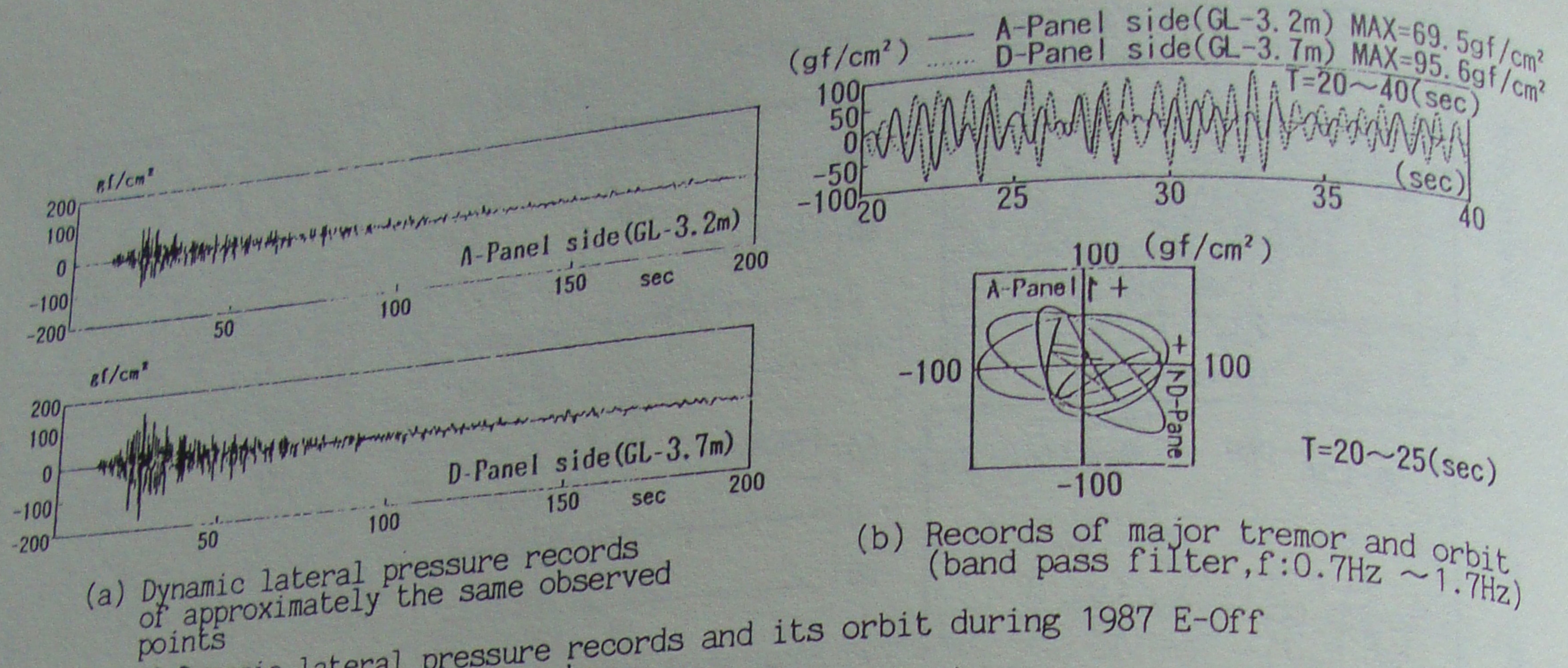


Fig. 12 Dynamic lateral pressure records and its orbit during 1987 E-Off Chiba Prefecture Earthquake (M=6.7, Focal depth=58km, Epicentral distance=75km)

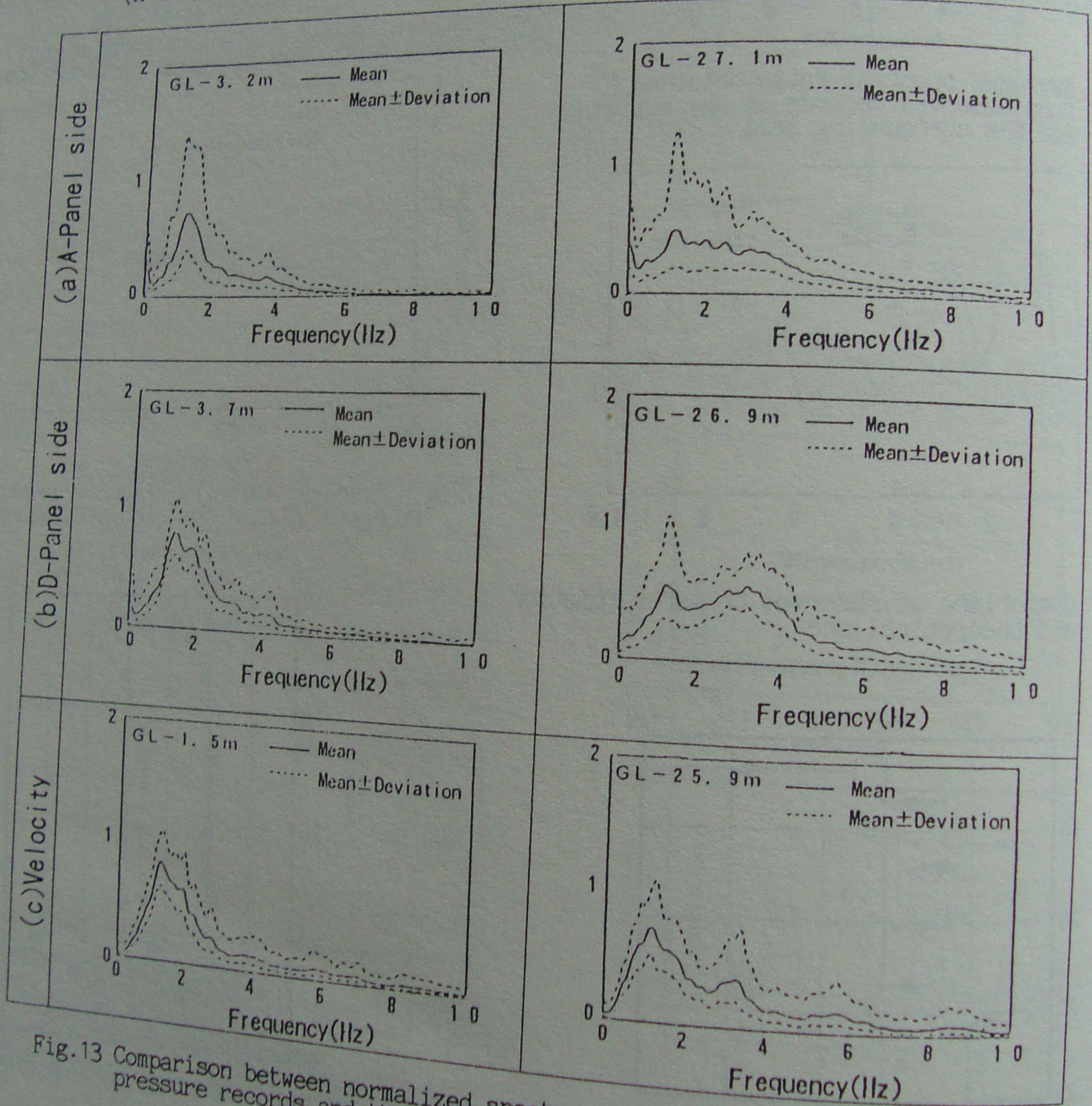


Fig. 13 Comparison between normalized spectra obtained from dynamic lateral pressure records and that obtained from velocity records